PROCEEDINGS OF SCIENCE

The Simplicity of Confinement

Xavier Crean[a], **Jeffrey Giansiracusa**[b] **and Biagio Lucini**[c,*]

[a] *Department of Mathematics, Faculty of Science and Engineering, Swansea University, Fabian Way, Swansea, SA1 8EN, UK*

[b] *Department of Mathematical Sciences, Durham University, Upper Mountjoy Campus, Durham, DH1 3LE, UK*

[c] *School of Mathematical Sciences, Queen Mary University of London, Mile End Road, London E1 4NS, United Kingdom*

E-mail: 2237451@swansea.ac.uk, jeffrey.giansiracusa@durham.ac.uk, b.lucini@qmul.ac.uk

We revisit the proposal that colour confinement is related to the dynamics of magnetic monopoles using methods derived from Topological Data Analysis, which provide a mathematically rigorous characterisation of topological properties of quantities defined on a lattice. After introducing homology, we discuss how this concept can be used to quantitatively analyse the behaviour of Abelian monopoles identified through the Maximal Abelian Projection across the deconfinement phase transition of SU(3) Yang-Mills. Specifically, we define an observable called "simplicity", which measures the number of connected components over the number of topologically non-trivial loops in a current network. A finite-size scaling analysis of the ensemble-averaged simplicity of Abelian magnetic monopole currents provides the expected value of the critical coupling with an accuracy that is generally higher than that obtained with conventional thermodynamic approaches at comparable statistics. Initial results for QCD are also discussed.

The 42nd International Symposium on Lattice Field Theory (LATTICE2025)
2-8 November 2025
Tata Institute of Fundamental Research, Mumbai, India

*Speaker

© Copyright owned by the author(s) under the terms of the Creative Commons Attribution-NonCommercial-NoDerivatives 4.0 International License (CC BY-NC-ND 4.0) All rights for text and data mining, AI training, and similar technologies for commercial purposes, are reserved. ISSN 1824-8039 . Published by SISSA Medialab.

PoS(LATTICE2025)190

1. Introduction and motivation

The absence of fractionally charged states in the asymptotic spectrum of Quantum Chromodynamics (QCD) – colour confinement – remains one of the most pressing open problems in our understanding of non-Abelian gauge theories. Lattice gauge theory continues to be among the most reliable frameworks for first-principles investigations of the phase structure of QCD (see Ref. [1] for a recent review). The commonly accepted scenario is that QCD has a confined and chirally broken regime at lower temperatures, and a quark-gluon plasma regime with chiral symmetry restored at higher temperatures. Recently, suggestions have been put forward that an intermediate region might exist in which chiral symmetry is restored while the system still displays confining features, see, e.g., Refs. [2–7]. Whether the boundaries of such an intermediate regime correspond to genuine phase transitions, and what their order is, can only be settled by an order parameter sensitive to the degrees of freedom that drive the dynamics.

A long-standing proposal identifies these degrees of freedom with magnetic monopoles condensing in the confining vacuum [8, 9], with the Abelian projection providing a convenient methodology to identify them [10]. On the lattice, this identification often employs the DeGrand and Toussaint proposal [11]. Magnetic charges in the projected theory organise themselves into closed current loops on the dual lattice, and a wealth of numerical evidence has accumulated for their relevance to the deconfinement transition (see, for instance, [12–14] and references therein). A robust order parameter built from these excitations that is free from lattice artefacts, accurate at moderate statistics, and applicable in the presence of dynamical fermions has so far remained elusive. A key obstacle is the intrinsically topological nature of monopole excitations, which is difficult to expose on a discrete lattice. Topological Data Analysis (TDA) has emerged in computational topology as a rigorous and robust methodology to characterise exactly topological features of discrete data, and its applications to field theory and statistical mechanics are growing rapidly (see, e.g., Refs. [15, 16] for recent work in this line of studies).

In this contribution, based on Ref. [17], which in turn builds on the earlier compact U(1) studies of Refs. [18, 19], we use TDA tools to construct a phase indicator[1] and test it in SU(3) Yang-Mills. The remainder of the write-up is organised as follows. Section 2 discusses Abelian monopole currents in the Maximal Abelian Gauge. Section 3 constructs the topological observable – the *simplicity* – as a ratio of Betti numbers of current graphs and discusses its properties in the two phases. Section 4 summarises the numerical setup and Section 5 reports our results. We conclude in Section 6 with an outlook that includes preliminary work towards full QCD.

2. Abelian monopoles in SU(3) Yang-Mills

We discretise SU(3) Yang-Mills theory on a four-dimensional Euclidean lattice of size $N_s^3 \times N_t$ with periodic boundary conditions, using the standard Wilson action

$$S = \beta \sum_i \sum_{\mu<\nu} \left[1 - \tfrac{1}{3} \operatorname{Re} \operatorname{Tr} U_{\mu\nu}(i) \right], \tag{1}$$

[1] We use this term over order parameter as the interpretation of our quantity in terms of the underlying symmetry is not immediate.

PoS(LATTICE2025)190

where $\beta = 6/g^2$, the $U_\mu(i) \in \mathrm{SU}(3)$ are link variables and $U_{\mu\nu}(i)$ is the plaquette. The temperature of the system is $T = 1/[a(\beta)\, N_t]$, with $a(\beta)$ the lattice spacing. The infinite-volume limit at fixed N_t is obtained by sending $N_s \to \infty$, and larger values of N_t result in finer lattice spacings at fixed temperature.

The identification of Abelian monopole currents proceeds via an Abelian projection: an operator transforming in the adjoint representation is diagonalised at each site and its eigenvalues are ordered, leaving a residual $\mathrm{U}(1)^{N-1}$ gauge symmetry. For SU(3) this exposes two species of monopoles. We work in the Maximal Abelian Gauge (MAG), in which gauge-invariant magnetic excitations are believed to overlap maximally with the projected ones [13]. Following Ref. [14], we define

$$\tilde{X}(i) = \sum_\mu \left[U_\mu(i)\, \tilde{\lambda}\, U_\mu^\dagger(i) + U_\mu^\dagger(i-\hat{\mu})\, \tilde{\lambda}\, U_\mu(i-\hat{\mu}) \right], \qquad \tilde{\lambda} = \mathrm{diag}(1,0,-1)\,, \tag{2}$$

and select the gauge in which $\tilde{X}(i)$ is diagonal at every site, equivalent to maximising

$$\tilde{F}_{\mathrm{MAG}}(U,g) = \sum_{\mu,i} \mathrm{tr}\Big[g(i)\, U_\mu(i)\, g^\dagger(i+\hat{\mu})\, \tilde{\lambda}\, g(i+\hat{\mu})\, U_\mu^\dagger(i)\, g^\dagger(i)\, \tilde{\lambda} \Big] \tag{3}$$

over the gauge transformations g. The MAG-fixed links are then projected over SU(3) diagonal matrices $\mathrm{diag}(e^{i\theta_1}, e^{-i(\theta_1-\theta_2)}, e^{-i\theta_2})$, with the angles θ_1 and θ_2 identifying the two monopole species. The DeGrand-Toussaint prescription [11] then assigns to each species an integer-valued current $m_\mu(j) \in \{0, \pm 1, \pm 2\}$ on the dual lattice Λ^*. By construction these currents are conserved at every dual site – the total charge entering a site equals the charge leaving it – so they cannot terminate and must form closed loops. Throughout this work, in line with Refs. [14, 19], we analyse the union of the two species on an equal footing, having verified that the two species individually yield statistically compatible results.

3. From current topology to the simplicity

For a given configuration, the set of dual links carrying a non-zero monopole current,

$$G = \left\{ (j;\hat{\mu}) \,:\, m_\mu(j) \neq 0 \right\}, \tag{4}$$

is naturally interpreted as a graph, whose vertices are the endpoints of the occupied links and whose edges are the links themselves. With $H_i(G)$ the i-th homology group of G, two topological invariants characterise the structure of the current network quantitatively:

- the zeroth Betti number $b_0 = \dim H_0(G)$, equal to the number of connected components of G;
- the first Betti number $b_1 = \dim H_1(G)$, equal to the number of independent loops of G, i.e. the number of edges left over after contracting a spanning forest of G.

Operationally, b_0 and b_1 can be computed efficiently with the GUDHI library [20]; further algorithmic details can be found in Ref. [18].

The behaviour of these two quantities averaged over ensembles at fixed temperature across the deconfinement transition is sketched in Fig. 1. At strong coupling (low temperature) large entropic fluctuations are favoured, and a typical configuration features a single percolating component

PoS(LATTICE2025)190

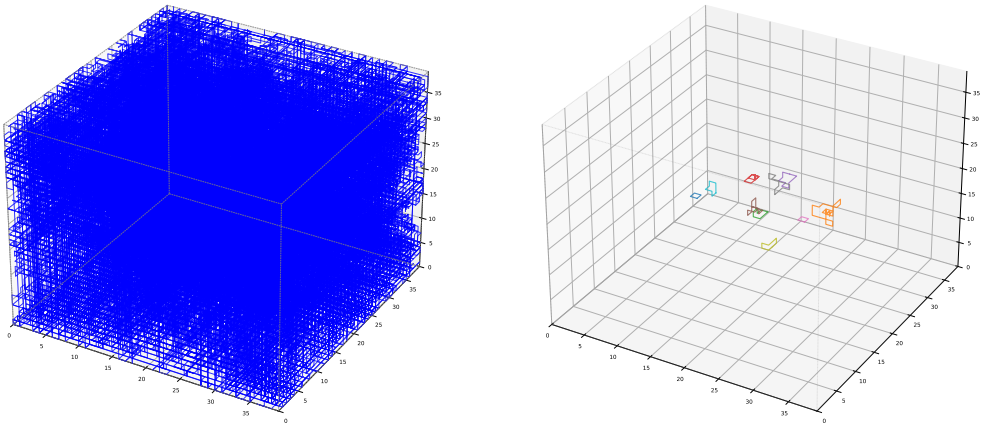

(a) Strong coupling (confined phase): one large percolating component carrying many independent loops, so that $b_0 \sim 1$ and $b_1 \gg 1$.

(b) Weak coupling (deconfined phase): a dilute gas of short, simple loops with $b_0 \sim b_1$.

Figure 1: Representative Abelian monopole current networks on the dual lattice, expected from SU(3) configurations on either side of the deconfinement transition. In the confined phase (a) the network is dominated by a single large, heavily looped component; in the deconfined phase (b) the Boltzmann suppression of long currents leaves a dilute collection of short, minimally looping components.

supporting many loops ($b_0 \sim 1$, $b_1 \gg 1$); at weak coupling (high temperature) the Boltzmann weight suppresses large structures and the network reduces to a dilute gas of small, minimally-looping clusters ($b_0 \sim b_1$). In Ref. [19] the densities

$$\rho_0 = \frac{\langle b_0 \rangle}{N_s^3}, \qquad \rho_1 = \frac{\langle b_1 \rangle}{N_s^3}, \tag{5}$$

and their susceptibilities χ_0, χ_1 were shown to be sensitive to the transition, with susceptibility peaks located at a pseudo-critical coupling $\beta_c(N_s, N_t)$ that, at fixed N_t, scales as

$$\beta_c(N_s, N_t) = \beta_c(N_t) + \frac{a_1}{N_s^3} + \dots, \tag{6}$$

the leading inverse-volume correction expected at a first-order transition. These results established a clear connection between the topology of the current graphs and deconfinement, but did not by themselves provide an order parameter.

Following the intuition represented in Fig. 1 we construct an order-parameter like observable combining the two Betti numbers into a single dimensionless observable, the *topological simplicity*

$$\lambda = \left\langle \frac{b_0}{b_1} \right\rangle . \tag{7}$$

The instantaneous ratio b_0/b_1 is the reciprocal of the number of homologically independent loops per connected component – the latter is sometimes called the *complexity*, and is at least 1, so that $b_0/b_1 \in (0, 1]$. At fixed N_t and in the thermodynamic limit, $\lambda \to 0$ in the confined phase, where a

PoS(LATTICE2025)190

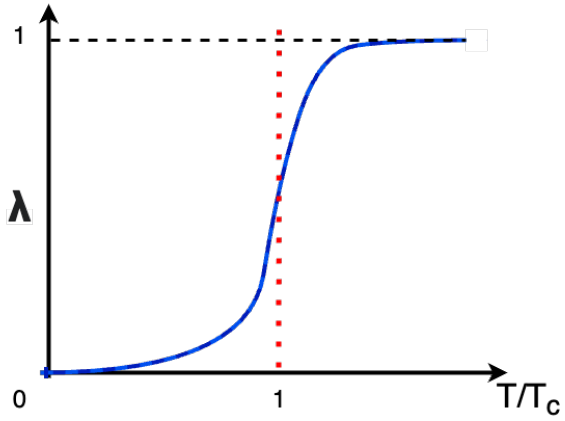

Figure 2: Sketch of the expected behaviour of the topological simplicity λ as a function of the reduced temperature T/T_c in the thermodynamic limit. The simplicity vanishes in the confined phase, approaches unity in the deconfined phase and, at a first-order transition, jumps across T_c. At finite volume the jump is smoothed into a steep rise, and the associated susceptibility develops a peak at T_c whose height grows with the volume.

single percolating component carries an extensive number of loops, while $\lambda \to 1$ in the deconfined phase, where almost every component is a single loop. Across the transition λ rises sharply from 0 to 1, as sketched in Fig. 2.

The sensitivity of λ to the transition is quantified by its susceptibility

$$\chi_\lambda = V\left(\left\langle\left(\frac{b_0}{b_1}\right)^2\right\rangle - \left\langle\frac{b_0}{b_1}\right\rangle^2\right), \qquad V = N_s^3, \tag{8}$$

which we expect to display a peak at the pseudo-critical coupling $\beta_c(N_s, N_t)$ obeying the scaling law (6).

4. Numerical setup

We have simulated SU(3) Yang-Mills at three temporal extents $N_t = 4, 6, 8$, each at five spatial extents respecting $N_s/N_t \geq 4$, over a window of β values strategically placed around the critical region known from Ref. [21]. Configurations are generated with a composite update made of one heat-bath [22] sweep followed by four over-relaxation sweeps; the first 10 000 composite updates are discarded for thermalisation and measurements are separated by 2 000 composite updates to suppress autocorrelations. Random numbers are produced with the RANLUX generator [23]. The ensemble parameters and the number of measured configurations $N_{\rm meas}$ per β value are summarised in Tab. 1.

For each configuration we fix the MAG by maximising $\tilde{F}_{\rm MAG}$ with an over-relaxed iterative procedure, identify the two Abelian projected gauge fields, and extract the corresponding monopole currents on Λ^*, from which we build the current graph G and compute b_0 and b_1. Thermal expectation values are estimated as sample means. The position of the susceptibility peaks is determined from the densely interpolated curves obtained by Ferrenberg-Swendsen multi-histogram reweighting [24], with statistical errors propagated through a bootstrap with $N_{\rm bs} = 2\,000$ resamples on effectively decorrelated subsamples of size $N_i^{\rm eff} = \lfloor N_i/\tau_i \rfloor$, τ_i being the integrated autocorrelation time at β_i.

PoS(LATTICE2025)190

N_t	N_s	$\beta_{\min}$	$\beta_{\max}$	N_β	N_{meas}
4	16, 20, 24, 28, 32	5.6600	5.7200	15	600
6	24, 30, 36, 42, 48	5.8100	5.9300	12	600
8	32, 40, 48, 56, 64	6.0350	6.0800	12	400

Table 1: Parameters of the lattice ensembles analysed in this work. For each (N_t, N_s) pair, N_{meas} configurations are recorded at each of N_β equally spaced values of β in $[\beta_{\min}, \beta_{\max}]$.

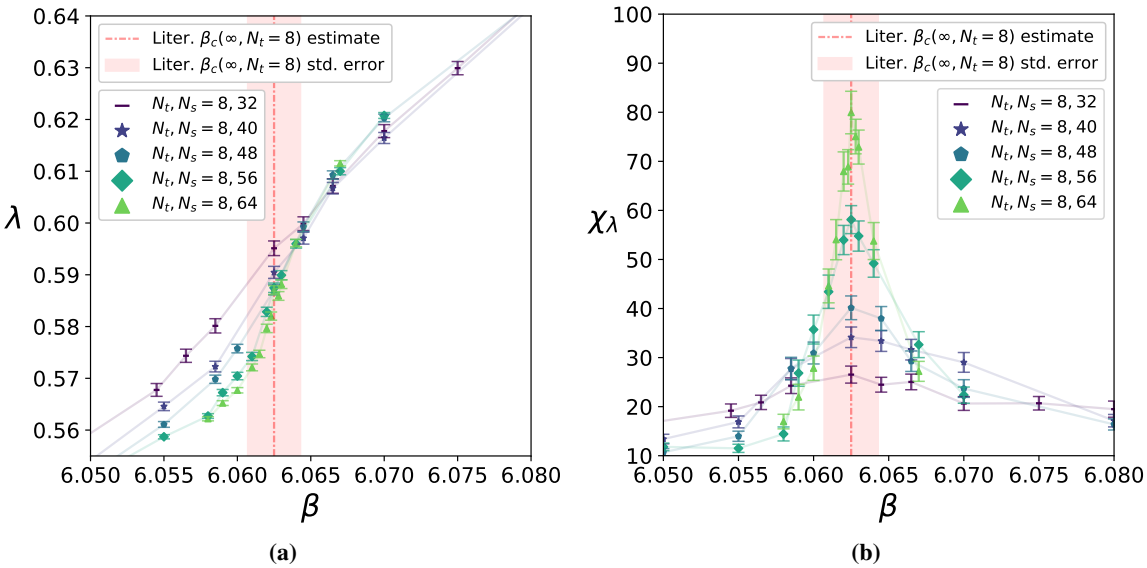

Figure 3: Simplicity λ (left) and its susceptibility χ_λ (right) as functions of β for $N_t = 8$ at five spatial volumes, in the neighbourhood of the deconfinement transition. Translucent lines guide the eye. The vertical red line and band show the central value and the 1σ band of β_c at $N_t = 8$ from the Polyakov-loop susceptibility of Ref. [21].

5. Results

Our results for the simplicity at $N_t = 8$ are reported in Fig. 3. The left panel shows λ as a function of β in the critical region: it rises monotonically, with a slope that steepens with the spatial volume and that, in the infinite-volume limit, is expected to become the sharp jump hinted in Fig. 2. The right panel shows the corresponding susceptibility χ_λ, which develops a clear peak in the critical region whose height grows and whose width shrinks as N_s increases – precisely the behaviour expected of an extensive observable at a first-order transition. Fully analogous behaviour is observed at $N_t = 4$ and $N_t = 6$ (not shown here; see Ref. [17]). The vertical band in both panels marks the literature value of β_c at $N_t = 8$ obtained from the finite-size scaling of the Polyakov-loop susceptibility [21], with which our peak positions are fully consistent.

The volume scaling of the position of the peak of χ_λ is shown in Fig. 4 for the coarsest ($N_t = 4$) and finest ($N_t = 8$) lattices analysed, the case $N_t = 6$ being entirely analogous. At each N_t we fit the data with the scaling law (6) and with a $1/N_s^6$ (i.e., quadratic in the spatial volume) correction, over

PoS(LATTICE2025)190

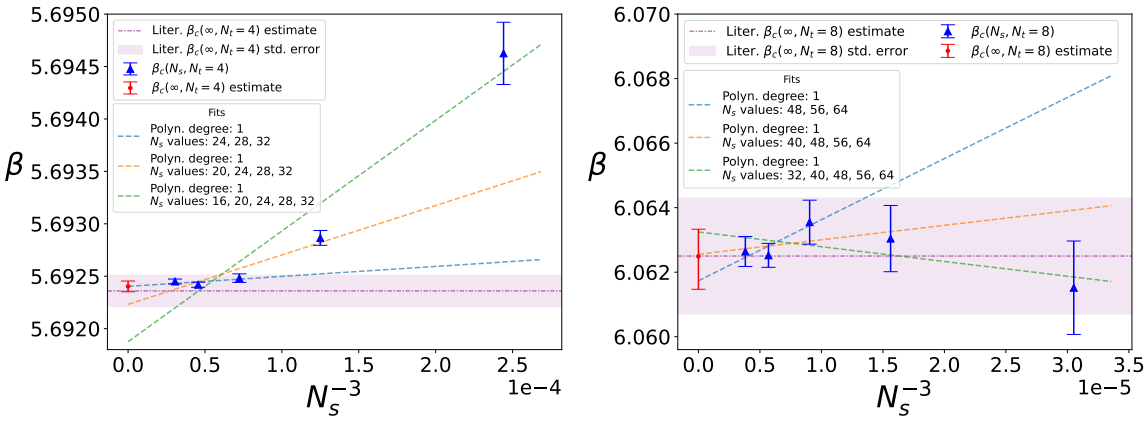

(a) $N_t = 4$ **(b)** $N_t = 8$

Figure 4: Infinite-volume extrapolation of the position of the peak of χ_λ at fixed N_t, shown for the coarsest ($N_t = 4$, left) and finest ($N_t = 8$, right) lattices analysed. Blue triangles are the bootstrap estimates of $\beta_c(N_s, N_t)$; dashed curves are individual polynomial fits in $1/N_s^3$; the red circle is the AIC-weighted infinite-volume estimate. The horizontal line and band give the corresponding determination of $\beta_c(N_t)$ from the Polyakov-loop susceptibility [21].

various fitting windows obtained by discarding the smallest volumes in turn. The individual fits are combined into a weighted ensemble following the Akaike-information-criterion (AIC) prescription of Ref. [25], which assigns to each fit a weight

$$w_i \propto \exp\left[-\tfrac{1}{2}\left(\chi_i^2 + 2\,n_{\mathrm{par},i} - n_{\mathrm{data},i}\right)\right], \tag{9}$$

favouring fits that combine a good description of the data, few parameters and the use of all available points. The infinite-volume estimate $\beta_c(N_t)$ and its 68% confidence interval are read off the cumulative distribution function of the resulting weighted Gaussian mixture.

The resulting estimates of β_c are collected in Tab. 2, together with the reference values from Ref. [21] obtained from the Polyakov-loop susceptibility. At each N_t our determinations agree with the literature value within errors, and the central values track the reference down to the fifth significant figure. Most notably, the statistical errors on the simplicity extrapolations are systematically smaller than those of the reference – by a factor of roughly two to three – even though the analysis of Ref. [21] used ensembles about an order of magnitude larger than ours[2]. This is strong evidence that λ is genuinely sensitive to the degrees of freedom that drive deconfinement.

6. Conclusions and outlook

We have proposed and tested a novel phase indicator for the deconfinement transition of SU(3) Yang-Mills theory, built from the topology of the Abelian monopole current networks identified in the Maximal Abelian Gauge. The observable – the *simplicity* $\lambda = \langle b_0/b_1 \rangle$ – is the reciprocal of the average number of homologically independent loops per connected component of the current graph;

[2]When the sweeps that separate measurements are taken into account, the statistics is found to be comparable. However, the conclusion that λ is found to be statistically more efficient persists.

PoS(LATTICE2025)190

	$N_t = 4$	$N_t = 6$	$N_t = 8$
β_c from λ (this work)	5.69240(5)	5.8940(4)	6.0625(10)
β_c from $\langle\lvert\bar{P}\rvert\rangle$ [21]	5.69236(15)	5.8941(12)	6.0625(18)

Table 2: Infinite-volume estimates of the critical coupling β_c from the simplicity of Eq. (7), compared with the determination from the modulus of the average Polyakov loop reported in Ref. [21]. The errors in the first row correspond to the 68% confidence interval of the AIC-weighted Gaussian mixture (symmetric within the quoted rounding); the asymmetric bounds are given in Ref. [17].

its definition involves only the dimensions of the homology groups of the graph, which are computed efficiently by standard cubical-complex libraries [20]. The simplicity interpolates between 0 in the confined phase and 1 in the deconfined phase, and its susceptibility exhibits the volume scaling expected at a first-order transition. A finite-size scaling analysis of χ_λ at $N_t = 4, 6, 8$ reproduces the known critical couplings of SU(3) Yang-Mills with a statistical accuracy markedly better than that of the Polyakov-loop determination at comparable statistics, despite the simplicity being the average of a ratio of integers rather than a thermodynamic derivative.

We note that λ remains well defined in the presence of dynamical fermions: Abelian magnetic current graphs and their homological properties can be extracted following the prescription provided here also for the theory with fermionic matter. Given our pure gauge results, we expect the simplicity to be sensitive to the upper boundary of an intermediate regime above the chiral crossover, should one exist: a non-monotonic structure of χ_λ at higher temperatures would be a clean qualitative signature. A first dedicated study of λ on the $N_f = 2 + 1$ FASTSUM Generation 2L ensembles of $O(a)$-improved Wilson fermions on anisotropic lattices [26] is in progress and shows a visible peak of χ_λ in the proposed second transition region that persists when the spatial volume is increased. Determining the features of this peak is the natural next step of the programme.

Acknowledgements

We thank G. Aarts, C. Allton and R. Bignell for the collaboration underpinning the results for full QCD discussed in this work. Moreover, we thank M. D'Elia, A. Gonzalez-Arroyo and T. Sulejmanpasic for discussions. XC was supported by the Additional Funding Programme for Mathematical Sciences, delivered by EPSRC (EP/V521917/1) and the Heilbronn Institute for Mathematical Research. JG was supported by EPSRC grant EP/R018472/1 through the Centre for TDA and by the Erlangen Hub for AI through EPSRC grant EP/Y028872/1. The work of BL was partly supported by the EPSRC ExCALIBUR ExaTEPP project EP/X017168/1 and by the STFC Consolidated Grants Nos. ST/T000813/1 and ST/X000648/1. Numerical simulations were performed on the Swansea SUNBIRD cluster (part of the Supercomputing Wales project) and on the AccelerateAI A100 GPU system, both part funded by the European Regional Development Fund via Welsh Government. This work used the DiRAC Data Intensive service (CSD3) at the University of Cambridge, managed by the University of Cambridge University Information Services on behalf of the STFC DiRAC HPC Facility (`www.dirac.ac.uk`). The DiRAC component of CSD3 at Cambridge was funded by BEIS,

PoS(LATTICE2025)190

UKRI and STFC capital funding and STFC operations grants. DiRAC is part of the UKRI Digital Research Infrastructure.

Research Software and Research Data Availability statement—The data and analysis code for this work are available at Ref. [27] and the Monte Carlo code at Ref. [28].

Use of AI statement—During the preparation of this work, the lead Author utilised Claude (Anthropic) to assist with literature search, document summarisation, background material synthesis and conceptual explanations.

References

[1] G. Aarts et al., *Phase Transitions in Particle Physics: Results and Perspectives from Lattice Quantum Chromo-Dynamics*, *Prog. Part. Nucl. Phys.* **133** (2023) 104070 [2301.04382].

[2] L.Y. Glozman, *$SU(2N_F)$ symmetry of QCD at high temperature and its implications*, *Acta Phys. Polon. Supp.* **10** (2017) 583 [1610.00275].

[3] A. Alexandru and I. Horváth, *Possible New Phase of Thermal QCD*, *Phys. Rev. D* **100** (2019) 094507 [1906.08047].

[4] M. Cardinali, M. D'Elia and A. Pasqui, *Thermal monopole condensation in QCD with physical quark masses*, 2107.02745.

[5] M. Hanada, H. Ohata, H. Shimada and H. Watanabe, *A New Perspective on Thermal Transition in QCD*, *PTEP* **2024** (2024) 041B02 [2310.01940].

[6] Y. Fujimoto, K. Fukushima, Y. Hidaka and L. McLerran, *New state of matter between the hadronic phase and the quark-gluon plasma?*, *Phys. Rev. D* **112** (2025) 074006 [2506.00237].

[7] J.A. Mickley, C. Allton, R. Bignell and D.B. Leinweber, *Novel insight into center-vortex geometry in four dimensions*, *Phys. Rev. D* **112** (2025) 054505 [2507.17200].

[8] S. Mandelstam, *Vortices and Quark Confinement in Nonabelian Gauge Theories*, *Phys. Rept.* **23** (1976) 245.

[9] G. 't Hooft, *Gauge theory for strong interactions*, in *New Phenomena in Subnuclear Physics*, A. Zichichi, ed., (Bologna), pp. 1225–1249, Editrice Compositori, 1976.

[10] G. 't Hooft, *Topology of the Gauge Condition and New Confinement Phases in Nonabelian Gauge Theories*, *Nucl. Phys. B* **190** (1981) 455.

[11] T.A. DeGrand and D. Toussaint, *Topological Excitations and Monte Carlo Simulation of Abelian Gauge Theory*, *Phys. Rev. D* **22** (1980) 2478.

[12] A.S. Kronfeld, M.L. Laursen, G. Schierholz and U.J. Wiese, *Monopole Condensation and Color Confinement*, *Phys. Lett. B* **198** (1987) 516.

[13] C. Bonati, A. Di Giacomo, L. Lepori and F. Pucci, *Monopoles, abelian projection and gauge invariance*, *Phys. Rev. D* **81** (2010) 085022 [1002.3874].

PoS(LATTICE2025)190

[14] C. Bonati and M. D'Elia, *The Maximal Abelian Gauge in SU(N) gauge theories and thermal monopoles for $N = 3$*, *Nucl. Phys. B* **877** (2013) 233 [1308.0302].

[15] N. Sale, J. Giansiracusa and B. Lucini, *Quantitative analysis of phase transitions in two-dimensional XY models using persistent homology*, *Phys. Rev. E* **105** (2022) 024121 [2109.10960].

[16] N. Sale, B. Lucini and J. Giansiracusa, *Probing center vortices and deconfinement in SU(2) lattice gauge theory with persistent homology*, *Phys. Rev. D* **107** (2023) 034501 [2207.13392].

[17] X. Crean, J. Giansiracusa and B. Lucini, *Simplicity of confinement in SU(3) Yang-Mills theory*, 2602.10088.

[18] X. Crean, J. Giansiracusa and B. Lucini, *Topological data analysis of monopole current networks in $U(1)$ lattice gauge theory*, *SciPost Phys.* **17** (2024) 100 [2403.07739].

[19] X. Crean, J. Giansiracusa and B. Lucini, *Topological Data Analysis of Abelian Magnetic Monopoles in Gauge Theories*, *PoS* **LATTICE2024** (2025) 395 [2501.19320].

[20] P. Dlotko, *Cubical complex*, in *GUDHI User and Reference Manual*, GUDHI Editorial Board (2015), http://gudhi.gforge.inria.fr/doc/latest/group__cubical__complex.html.

[21] B. Lucini, M. Teper and U. Wenger, *The High temperature phase transition in SU(N) gauge theories*, *JHEP* **2004** (2004) 061 [hep-lat/0307017].

[22] N. Cabibbo and E. Marinari, *A New Method for Updating SU(N) Matrices in Computer Simulations of Gauge Theories*, *Phys. Lett. B* **119** (1982) 387.

[23] M. Luscher, *A Portable high quality random number generator for lattice field theory simulations*, *Comput. Phys. Commun.* **79** (1994) 100 [hep-lat/9309020].

[24] A.M. Ferrenberg and R.H. Swendsen, *Optimized Monte Carlo analysis*, *Phys. Rev. Lett.* **63** (1989) 1195.

[25] W.I. Jay and E.T. Neil, *Bayesian model averaging for analysis of lattice field theory results*, *Phys. Rev. D* **103** (2021) 114502 [2008.01069].

[26] FASTSUM collaboration, *Open charm mesons at nonzero temperature: results in the hadronic phase from lattice QCD*, 2209.14681.

[27] X. Crean, J. Giansiracusa and B. Lucini, *Simplicity of confinement in $SU(3)$ Yang-Mills theory — Data and Analysis Code Release*, 2026. 10.5281/zenodo.18395360.

[28] X. Crean, J. Giansiracusa and B. Lucini, *Simplicity of confinement in $SU(3)$ Yang-Mills theory — Monte Carlo Code Release*, 2026. 10.5281/zenodo.18171195.

PoS(LATTICE2025)190